

**INTERPRETATION OF CIRRUS CLOUD PROPERTIES USING COINCIDENT
SATELLITE AND LIDAR DATA DURING THE FIRE CIRRUS IFO**

Patrick Minnis and Joseph M. Alvarez
Atmospheric Sciences Division, NASA Langley Research Center
Hampton, Virginia 23665-5225

David F. Young
Aerospace Technologies Division, Planning Research Corporation
Hampton, Virginia 23666

Kenneth Sassen
Department of Meteorology, University of Utah
Salt Lake City, Utah 84112

Christian J. Grund
Department of Meteorology, University of Wisconsin
Madison, Wisconsin 53702

1. Introduction

The First ISCCP Regional Experiment (FIRE) Cirrus Intensive Field Observations (IFO) provide a unique opportunity to examine the relationships between the satellite-observed radiances and various parameters which describe the bulk properties of clouds, such as cloud amount and cloud-top height. In this paper, lidar-derived cloud altitude data, radiosonde data, and satellite-observed radiances are used to examine the relationships between visible reflectance, infrared emittance, and cloud-top temperatures for cirrus clouds.

2. Data

Lidar backscatter data taken over Ft. McCoy (FMC), Wausau, and Madison, Wisconsin during the FIRE Cirrus IFO (October 19 - November 2, 1986) were used to define the cloud base, cloud-top altitude z_t , cloud thickness h , and effective cloud center altitude z_c . The last parameter is based on the distribution of backscatter intensity. Sassen et al. (1989) discuss the instrumentation and measurements in more detail. Soundings from Green Bay, Wisconsin, were used to determine the temperature-height relationships for all of the data. Cloud-top temperature T_t corresponds to z_t on the soundings. Mean cloud-center temperature T_c is found from z_c . Surface temperatures were used to supplement the clear-sky temperatures T_{cs} derived from the satellite data. Half-hourly VIS ($0.65\mu\text{m}$) and IR ($11.5\mu\text{m}$), 4-km data from the Geostationary Operational Environmental Satellite (GOES) were extracted along the wind vector at z_c for areas 4-pixels wide and ~ 16-pixels long. The VIS data were converted to reflectance ρ using the calibration of C. H. Whitlock (1988, personal communication). Clear-sky temperature is derived for each data strip whenever some clear pixels are observed in the VIS data. Otherwise, alternate methods are used to compute

T_{cs} . For all pixels (denoted as cloudy pixels) having an equivalent blackbody temperature, $T < T_{cs} - 3K$, the effective cloud beam emittance is

$$\epsilon = \{ [B(T) - B(T_{cs})] / [B(T_z) - B(T_{cs})] \}, \quad (1)$$

where T_z refers to the temperature at altitude z . The emittance is calculated twice for each satellite data strip using T_c and T_t in place of T_z . It is also assumed that

$$\epsilon = 1 - \exp(-\tau_e / \mu), \quad (2)$$

where the cloud IR optical depth is τ_e and μ is cosine of the viewing zenith angle. The cloud reflectance, ρ_c , is assumed to be related to the observed reflectance in the following manner.

$$\rho = T_a \rho_c + \rho_s T_c T_u + \alpha_{sd}(1 - \alpha_d)(1 - T_c - \alpha_c), \quad (3)$$

where T_a is the transmittance of the atmosphere above the cloud; T_c and T_u are the transmittances of the cloud to downward and upward direct radiation, respectively; ρ_s and α_{sd} are the clear-sky bidirectional reflectance and diffuse albedos, respectively; and α_d and α_c are the albedos of the cloud to diffuse and total radiation, respectively. Thus, $\alpha_d = \alpha_d(\tau_v)$; $\alpha_c = \alpha_c(\tau_v, \mu_0)$; and $\rho_c = \chi_c \alpha_c$. The cosine of the solar zenith angle is μ_0 . It is assumed that the anisotropic reflectance correction factor χ_c is independent of the VIS optical depth τ_v . Values for χ_c are taken from the empirical model of Minnis and Harrison (1984). The relationship between τ_v and cloud albedo is based on the results of Takano and Liou (1989) for a cloud containing randomly oriented hexagonal ice columns 125 μm long and 50 μm wide. Cloud transmittance also depends on the VIS optical depth. Mean values of T were computed for each discrete reflectance value.

In the ISCCP methodology, the scattering ratio, r , is used to relate the VIS optical depth to τ_e in order to correct for the semitransparency of the cloud. This quantity is equivalent to τ_v / τ_e . It is calculated here as

$$r = \frac{\sum_{i=1}^N (\tau_v / \tau_e)_i}{N},$$

where N is the number of cloudy pixels for each data strip. Details concerning the data and methodology are given by Minnis et al. (1989).

3. Results and Discussion

Figure 1 shows an example of the observed values of ϵ , ρ , and α_c for cirrus clouds over FMC at 15 UTC, October 28, 1986. Averaging the temperatures minimizes some of the noise introduced by cloud structure variations. Mean values of r computed at each half hour for the cirrus days during the IFO (October 22, 27, 28, and 30; November 1 and 2) are summarized in Table 1. It is expected that r is constant for a given cirrus cloud. Thus, the systematic variation of r with scattering angle θ indicates that the values of χ_c used here are inadequate. The mean value of $r = 2.1$, however, is very close to the value of 2.0 expected for large-particle clouds (e.g., Hansen and Travis, 1974). Assuming that the computed mean value of r is correct, it is possible to compute more realistic values of χ_c by forcing the results to yield $r = 2.1$ for each data strip. The average values of χ_c resulting from this process are shown as the dashed lines in Fig. 2. Obviously, the cirrus clouds scatter radiation more anisotropically than the average cloud. Optically thin clouds tend to mimic the single-scattering phase function. Optically thick clouds tend to reduce anisotropy through multiple scattering. Scattering ratios from Table 1 averaged according to T_c are shown in Fig. 3. The average values of r are 2.5 ± 0.2 for $T_c < 235$ K and 1.9 ± 0.2 for $T_c > 235$ K. The larger values of r are significantly different from 2.0 suggesting that the colder clouds contain a substantial number of small particles. The temperature dependency of r is similar to that found by Platt and Dilley (1981). The variation of cloud emittance (corrected for μ) with T_c given in Fig. 4 for the case study (October 27-28) is much like that determined by Platt et al. (1987) from ground observations. The data for the entire period, however, show greater increases of ϵ with temperature than found by Platt et al. (1987). Cloud thickness (Fig. 5) during the case study is also similar to the Platt et al. (1987) results. Ratios of $\epsilon(T_t) / \epsilon(T_c)$ are plotted against T_c in Fig. 6. The nearly linear dependency of these ratios on T_c indicates that the actual cloud-top temperature can be determined if T_c is found first. Other results from these analyses (Minnis et al., 1989) indicate that cloud shadows have a significant effect on the retrieved cloud albedos. This shadowing can result in "dark" pixels which are colder than T_{cs} and darker than ρ_s . Their effects must be considered in the retrieval of cirrus properties from VIS and IR data.

4. Concluding Remarks

The analysis of IFO data shows consistency with earlier cirrus studies suggesting that some simple parameterizations of cirrus cloud properties can be effectively utilized. Other results indicate that additional parameters may be derived from the satellite data. More cases taken over other areas will be needed to confirm the results presented here.

REFERENCES

- Hansen, J. E. and L. D. Travis, 1974: Light scattering in planetary atmospheres. Space Sci. Rev., 16, 527-610.
- Minnis, P., and E. F. Harrison, 1984: Diurnal variability of regional cloud and clear-sky radiative parameters derived from GOES data, Part III: November 1978 radiation parameters. J. Clim. Appl. Meteor., 23, 1032-1051.
- Minnis, P., D. F. Young, K. Sassen, J. M. Alvarez, and C. J. Grund, 1989: The 27-28 October 1986 FIRE Cirrus IFO case study: Cirrus parameter relationships derived from satellite and lidar data. Submitted to Mon. Wea. Rev.
- Platt, C. M. R., and A. C. Dilley, 1981: Remote sounding of high clouds: IV. Observed temperature variations in cirrus optical properties. J. Atmos. Sci., 38, 1069-1082.
- Platt, C. M. R., J. C. Scott, and A. C. Dilley, 1987: Remote sounding of high clouds, VI. Optical properties of midlatitude and tropical cirrus. J. Atmos. Sci., 44, 729-747.
- Sassen, K., C. J. Grund, J. Spinhirne, M. Hardesty, and J. M. Alvarez, 1989: The 27-28 October 1986 FIRE IFO cirrus case study: A five lidar view of cirrus cloud structure and evaluation. Submitted to Mon. Wea. Rev.
- Takano, Y. and K. N. Liou, 1989a: Radiative transfer in cirrus clouds: II. Theory and computation of multiple scattering in an anisotropic medium. J. Atmos. Sci., 46, 21-38.

UTC	Cases (IFO)	θ ($^\circ$)	All Data (IFO) τ_v	r	Case Study τ_v	r
1330	4	109	0.97	1.08	0.15	0.85
1400	3	117	1.84	1.42	0.17	1.19
1430	2	124	0.90	1.76	0.31	1.68
1500	3	131	1.46	2.01	1.46	2.01
1600	5	146	2.31	2.22	1.72	1.98
1630	2	153	2.44	1.74	---	---
1700	6	160	1.78	2.99	1.39	2.94
1800	6	173	2.20	3.49	1.94	5.65
1830	1	175	3.52	1.98	---	---
1900	7	168	2.50	2.81	0.63	3.13
1930	4	162	1.52	2.73	0.74	2.76
2000	8	154	1.93	2.68	1.28	3.06
2030	5	147	1.40	2.47	1.63	2.34
2100	6	140	1.06	1.99	0.97	2.46
2130	4	132	1.15	1.30	0.53	1.20
2200	5	125	0.67	0.83	0.28	0.68
totals and means	71	---	1.69	2.08	1.04	2.07

Table 1. Reflectance parameters computed for all data.

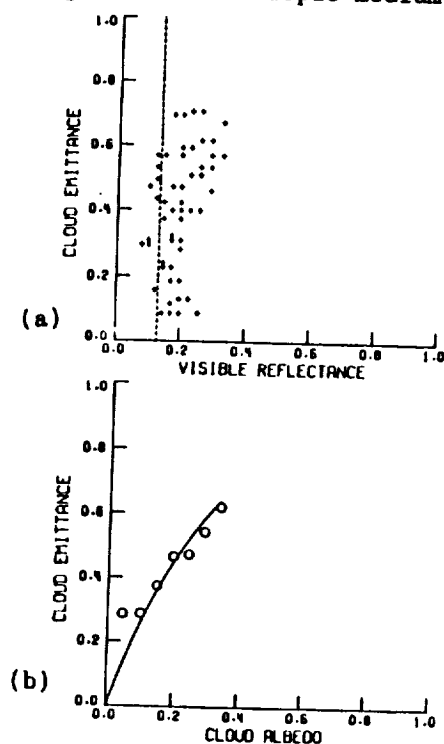


Fig. 1. Cloud emittances and observed (a) reflectances and (b) cloud albedos for cirrus clouds over FMC at 1500 UTC, October 28, 1986.

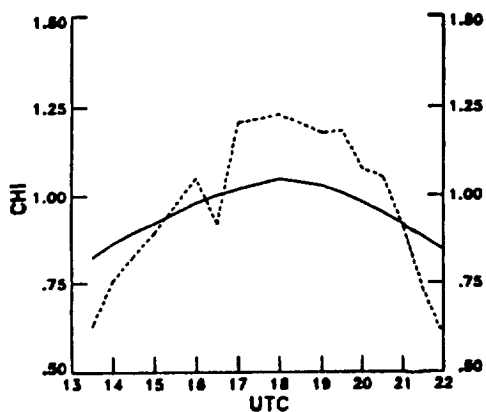


Fig. 2. Mean anisotropic reflectance correction factors for the IFO. The solid line is the nominal model; the dashed line represents the values derived for $r = 2.1$.

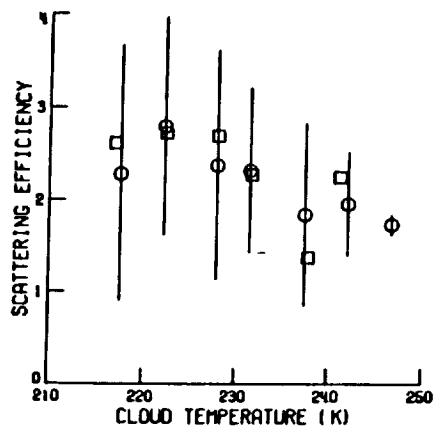


Fig. 3. Variation of mean scattering ratio with cloud-center temperature.

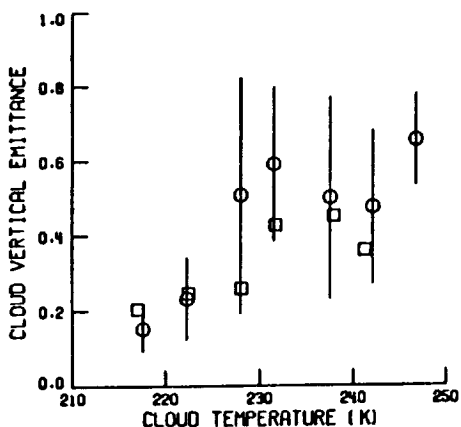


Fig. 4. Variation of cloud vertical beam emittance with cloud-center temperature.

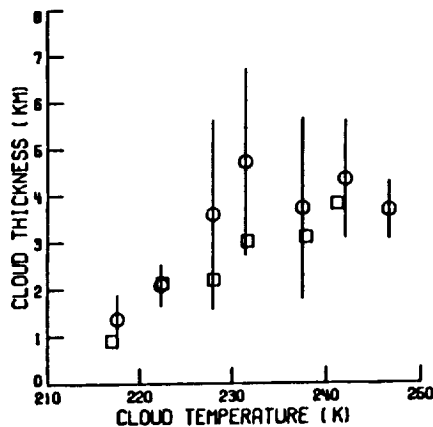


Fig. 5. Dependence of cloud thickness on cloud-center temperature.

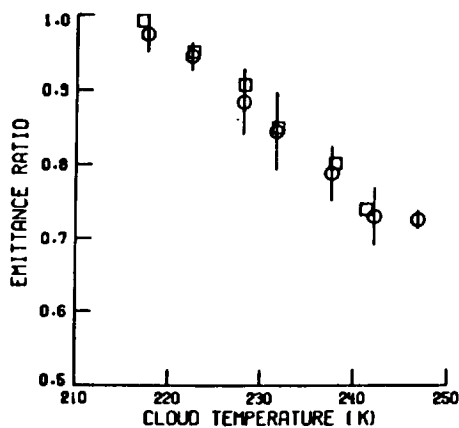


Fig. 6. Variation of emittance ratio with cloud-center temperature.

